Electronic Supplementary Material (ESI) for Journal of Materials Chemistry C.

Electronic supplementary information

Columnar liquid-crystalline assemblies of X-shaped pyrene-oligothiophene conjugates: Photoconductivities and mechanochromic functions

Kian Ping Gan, Masafumi Yoshio* and Takashi Kato*

1. Experimental

General methods

All materials were purchased from Tokyo Chemical Industry (TCI), Sigma Aldrich, Wako Pure Chemical Industry, or Kanto Chemical Industry. All reactions were carried out under an argon atmosphere unless otherwise stated. Silica gel column chromatography was performed with silica gel 60 from Kanto Chemicals (spherical 40–50 μm). ^{1}H and ^{13}C NMR spectra were recorded on a JEOL ECX-400. Chemical shifts of ^{1}H and ^{13}C signals are expressed in parts per million (δ) using internal standards Me_4Si (δ = 0.00) and $CHCl_3$ (δ = 77.00), respectively. Coupling constants (*J*) are reported in Hertz (Hz). Mass spectra (MALDI-TOF) were recorded on a Bruker Autoflex Speed TOF, with *trans*-2-[3-(4-tert-Butylphenyl)-2-methyl-2-propenylidene]malononitrile as the matrix. Elemental analyses were carried out on an Exeter Analytical CE-440 Elemental Analyser.

4-Bromo-1,2-bis(dodecyloxy)benzene **2a**,[1] and 5-bromo-1,2,3-tri(dodecyloxy)benzene **2b**,[2] were synthesised based on previously reported procedures. Compounds **6**, [3, 4] and **7**,[5] were previously reported as gelators for common organic solvents.

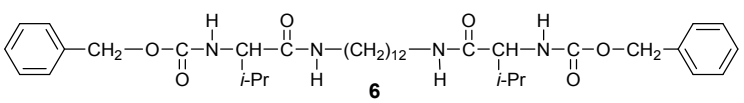

6

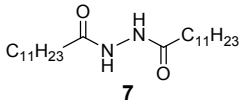

7

5-(3,4-bis(dodecyloxy)phenyl)-2,2'-bithiophene (3a)

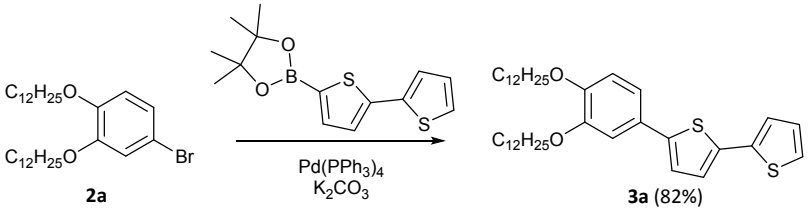

2a **3a** (82%)

An argon-degassed solution of THF (50 ml) and water (10 ml) was added to a mixture of K_2CO_3 (3.37 g, 24.4 mmol), 4-bromo-1,2-bis(dodecyloxy)benzene **2a** (8.00 g, 15.2 mmol), 2,2'-bithiophene-5-boronic acid pinacol ester (4.90 g, 16.8 mmol), and $Pd(PPh_3)_4$ (880 mg, 0.76 mmol) at room temperature. The resulting mixture was stirred at 70 ˚C for 16 hours under an argon atmosphere. The reaction mixture was then cooled, diluted with water, and then extracted with dichloromethane 3 times. The organic layer was washed with brine and dried with $MgSO_4$. After filtration and concentration *in vacuo*, the crude product was then filtered through a silica gel plug (eluent: hexane/ dichloromethane = 5/5). Subsequent recrystallization from hexane/ ethanol = 1/9 afforded flaky yellow solid **3a** (7.60 g, 12.4 mmol, 82%). ^{1}H NMR (400 MHz, $CDCl_3$) δ = 7.19 (dd, *J* = 5.2 Hz, 1.6 Hz, 1H), 7.17 (dd, *J* = 3.6 Hz, 1.2 Hz, 1H), 7.14-7.08 (m, 4H), 7.01 (dd, *J* = 5.6 Hz, 3.6 Hz, 1H), 6.87 (d, *J* = 8.4 Hz, 1H), 4.06-3.99 (m, 4H), 1.87-1.78 (m, 4H), 1.50-1.43 (m, 4H), 1.40-1.22 (br, 32H), 0.89-0.86 (m, 6H).^{13}C NMR (100 MHz, $CDCl_3$) δ = 149.5, 149.2, 143.5, 137.7, 135.8, 127.9, 127.3, 124.6, 124.2, 123.4, 122.8, 118.6, 114.1, 111.8, 69.5, 69.5, 32.0, 29.8, 29.7, 29.5, 29.5, 29.4, 26.1, 22.8, 14.2.

5'-(3,4,5-tris(dodecyloxy)phenyl)-2,2'-bithiophene (3b)

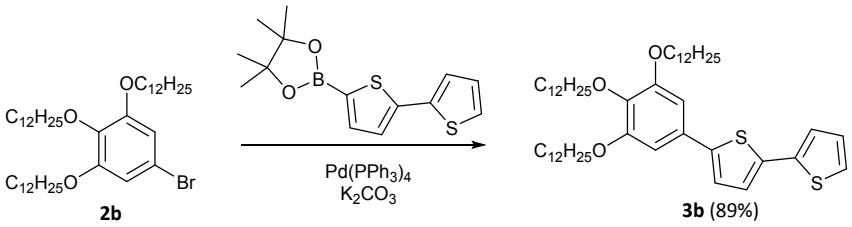

An argon-degassed solution of THF (30 ml) and water (6 ml) was added to a mixture of K_2CO_3 (1.61 g, 11.63 mmol), 5-bromo-1,2,3-tri(dodecyloxy)benzene **2b** (5.56 g, 7.83 mmol), 2,2'-bithiophene-5-boronic acid pinacol ester (2.38 g, 8.13 mmol), and $Pd(PPh_3)_4$ (451 mg, 0.39 mmol) at room temperature. The resulting mixture was stirred at 70 ˚C for 12 hours under an argon atmosphere. The reaction mixture was then cooled, diluted with water, and then extracted with dichloromethane 3 times. The organic layer was washed with brine and dried with $MgSO_4$. After filtration and concentration *in vacuo*, the crude product was then filtered through a silica gel plug (eluent: hexane/ dichloromethane = 3/7). Subsequent recrystallization from ethyl acetate/ ethanol = 2/8 afforded pale yellow solid **3b** (5.57 g, 7.00 mmol, 89%). ^{1}H NMR (400 MHz, $CDCl_3$) δ = 7.21 (dd, *J* = 5.2 Hz, 1.2 Hz, 1H), 7.18 (dd, *J* = 3.6 Hz, 1.2 Hz, 1H), 7.11 (s, 2H), 7.02 (dd, *J* = 7 Hz, 4 Hz, 1H), 6.76 (s, 2H), 4.02 (t, *J* = 6.8 Hz, 4H), 3.97 (t, *J* = 6.8 Hz, 2H), 1.85-1.71 (m, 6H), 1.52-1.45 (m, 6H), 1.40-1.22 (br, 48H), 0.874 (t, *J* = 6.8 Hz, 9H). ^{13}C NMR (100 MHz, $CDCl_3$) δ = 153.5, 143.6, 138.4, 137.6, 136.3, 129.4, 127.9, 124.5, 124.3, 123.5, 123.4, 104.7, 73.7, 69.4, 32.0, 30.4, 29.9, 29.8, 29.8, 29.5, 29.5, 26.2, 22.8, 14.2.

(5'-(3,4-bis(dodecyloxy)phenyl)-[2,2'-bithiophen]-5-yl)boronic acid pinacol ester (4a)

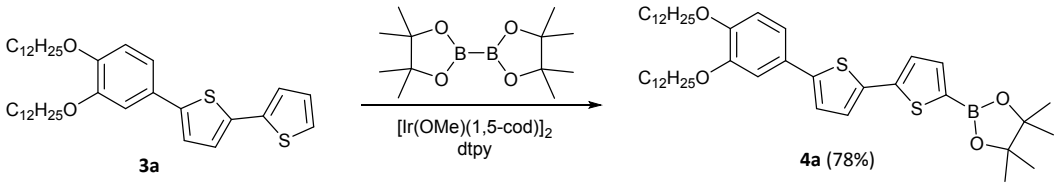

An argon-degassed solution of hexane (50 ml) was added to a mixture of 5-(3,4-bis(dodecyloxy)phenyl)-2,2'-bithiophene **3a** (4.37 g, 7.15 mmol), bis(pinacolato)diboron (B_2Pin_2) (2.00 g, 7.88 mmol), 4,4'-di-tert-butyl-2,2'-dipyridyl (dtpy) (77 mg, 0.29 mmol), and (1,5-cyclooctadiene)(methoxy)iridium(I) dimer ($[Ir(OMe)(1,5\text{-}cod)]_2$) (95 mg, 0.14 mmol), the resulting mixture was stirred at room temperature for 24 hours. The reaction mixture was then concentrated *in vacuo*, followed by purification by silica gel column chromatography (eluent: hexane/ ethyl acetate = 4/6). Subsequent recrystallization from ethanol afforded brownish green solid of **4a** (4.10 g, 5.56 mmol, 78%). ^{1}H NMR (400 MHz, $CDCl_3$) δ = 7.52 (d, *J* = 3.6 Hz, 1H), 7.23 (d, *J* = 3.6 Hz. 1H), 7.17 (d, *J* = 4 Hz, 1H), 7.133-7.09 (m, 3H), 6.87 (d, *J* = 8.4 Hz, 1H), 4.06-3.99 (m, 4H), 1.87-1.78 (m, 4H), 1.53-1.43 (m, 4H), 1.39-1.22 (br, 41H), 0.89-0.85 (m, 6H). ^{13}C NMR (100 MHz, $CDCl_3$) δ = 149.4, 149.3, 144.4, 144.2, 138.1, 135.6, 127.2, 125.3, 124.6, 123.0, 118.7, 114.1, 111.8, 84.3, 69.4, 32.0, 29.8, 29.7, 29.5, 26.1, 24.9, 22.8, 14.2.

(5'-(3,4,5-tris(dodecyloxy)phenyl)-[2,2'-bithiophen]-5-yl)boronic acid pinacol ester (4b)

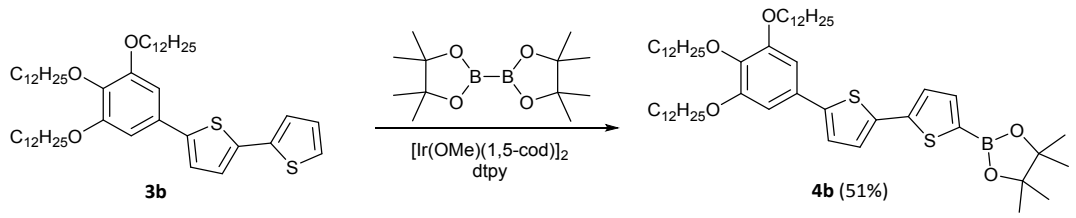

An argon-degassed solution of hexane (50 ml) was added to a mixture of 5'-(3,4,5-tris(dodecyloxy)phenyl)-2,2'-bithiophene **3b** (5.0 g, 6.29 mmol), bis(pinacolato)diboron (B_2Pin_2) (1.76g, 6.92 mmol), 4,4'-di-tert-butyl-2,2'-dipyridyl (dtpy) (68 mg, 0.25 mmol) and (1,5-cyclooctadiene)(methoxy)iridium(I) dimer ($[Ir(OMe)(1,5\text{-}cod)]_2$) (83 mg, 0.13 mmol). The resulting mixture was stirred at room temperature for 24 hours. The reaction mixture was then concentrated *in vacuo*, followed by purification by silica gel column chromatography twice (eluent: hexane/ dichloromethane = 4/6), to afford viscous green liquid of **4b** that was solidified on standing. (2.95 g, 3.20 mmol, 51%). ^{1}H NMR (400 MHz, $CDCl_3$) δ = 7.53 (d, *J* = 3.6 Hz, 1H), 7.24 (d, *J* = 3.6 Hz, 1H), 7.17 (d, *J* = 3.6 Hz, 1H), 7.12 (d, *J* = 4.4 Hz, 1H), 6.77 (s, 2H), 4.04-3.96 (m, 6H), 1.86-1.73 (m, 6H), 1.51-1.45 (m, 6H), 1.41-1.20 (br, 57H), 0.90-0.87 (m, 9H). ^{13}C NMR (100 MHz, $CDCl_3$) δ = 153.5, 144.3, 138.4, 138.1, 136.1, 129.3, 125.2, 124.7, 123.6, 104.8, 84.3, 73.7, 69.3, 32.0, 30.5, 29.9, 29.8, 29.8, 29.5, 26.2, 24.9, 22.8, 14.2.

1,3,6,8-tetrakis(5'-(3,4-bis(dodecyloxy)phenyl)-[2,2'-bithiophen]-5-yl)pyrene (1a)

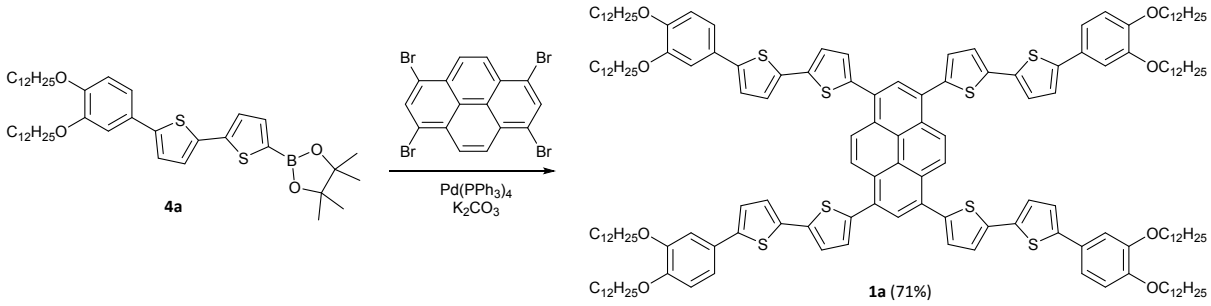

An argon-degassed solution of THF (30 ml) and water (5 ml) was added to a mixture of K_2CO_3 (1.00 g, 4.62 mmol), 1,3,6,8-tetrabromopyrene (409 mg, 0.79 mmol), (5'-(3,4-bis(dodecyloxy)phenyl)-[2,2'-bithiophen]-5-yl)boronic acid pinacol ester (**4a**) (2.60 g, 3.53 mmol), and $Pd(PPh_3)_4$ (222 mg, 0.19 mmol) at room temperature. The resulting mixture was stirred at 70 ˚C for 30 hours under an argon atmosphere. The reaction mixture was cooled, diluted with water, and then extracted with dichloromethane 3 times. The organic layer was washed with brine and dried with $MgSO_4$. After filtration and concentration *in vacuo*, the crude product was then purified by silica gel column chromatography twice (eluent: hexane/ dichloromethane = 5/5). The dark red solid was then dissolved in hot hexane/ ethanol = 8/2, cooled in a fridge and precipitation was then induced by the addition of ethanol. The mixture was then filtered, washing with ethanol to afford bright red powder of **1a** (1.49 g, 0.56 mmol, 71%). ^{1}H NMR (400 MHz, $CDCl_3$) δ = 8.61 (s, 4H), 8.27 (s, 2H), 7.32 (d, *J* = 4 Hz, 4H), 7.31 (d, *J* = 3.6 Hz, 4H), 7.2 (d, *J* = 4 Hz, 4H), 7.17-7.13 (m, 12H), 6.88 (d, *J* = 8 Hz, 4H), 4.07-4.00 (m, 16H), 1.87-1.81 (m, 16H), 1.52-1.43 (m, 16H), 1.41-1.20 (br, 128H), 0.87-0.85 (m, 24H). ^{13}C NMR (100 MHz, $CDCl_3$) δ = 149.5, 149.3, 143.8, 140.5, 139.0, 135.5, 129.6, 128.9, 127.3, 126.2, 125.8, 124.8, 123.9, 123.0, 118.6, 114.1, 111.7, 69.5, 69.5, 32.0, 29.8,

29.8, 29.6, 29.5, 29.4, 29.4, 26.1. MS (MALDI-TOF): cald for [M^+]: 2636.57; found: 2636.56. Elemental Analysis cald (%) for $C_{168}H_{234}O_8S_8$: C, 76.49; H, 8.94; found: C, 76.75; H, 9.04.

1,3,6,8-tetrakis(5'-(3,4,5-tris(dodecyloxy)phenyl)-[2,2'-bithiophen]-5-yl)pyrene (1b)

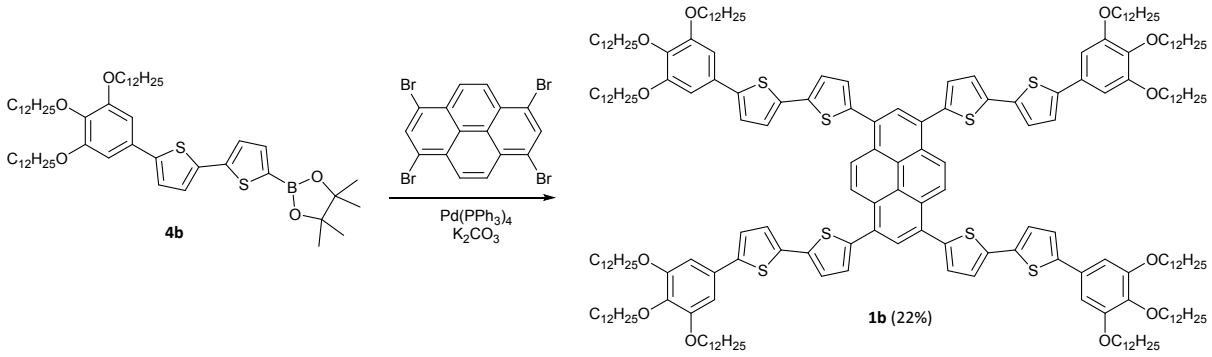

An argon-degassed solution of THF (30 ml) and water (5 ml) was added to a mixture of K_2CO_3 (500 mg, 3.62 mmol), 1,3,6,8-tetrabromopyrene (311 mg, 0.60 mmol), (5'-(3,4,5-tris(dodecyloxy)phenyl)-[2,2'-bithiophen]-5-yl)boronic acid pinacol ester (**4b**) (2.50 g, 2.71 mmol), and $Pd(PPh_3)_4$ (139 mg, 0.12 mmol) at room temperature. The resulting mixture was stirred at 70 ˚C for 30 hours under an argon atmosphere. The reaction mixture was then cooled, diluted with water, and then extracted with dichloromethane 3 times. The organic layer was washed with brine and dried with $MgSO_4$. After filtration and concentration *in vacuo*, the crude product was then purified by silica gel column chromatography twice (eluent: hexane/ dichloromethane = 5/5). The dark red solid was then dissolved in hot hexane/ ethanol = 8/2, cooled in a fridge, and precipitation was then induced with the addition of ethanol. The mixture was then filtered, washing with ethanol to afford bright red powder of **1b** (446 mg, 0.13 mmol, 22%). ^{1}H NMR (400 MHz, $CDCl_3$) δ = 8.64 (s, 4H), 8.29 (s, 2H), 7.34 (m, 8H), 7.21 (d, *J* = 4.4 Hz, 4H), 7.16 (d, *J* = 3.6 Hz, 4H), 4.06-3.97 (m, 24H), 1.87-1.74 (m, 24H), 1.51-1.46 (m, 25H), 1.45-1.26 (br, 192H), 0.9-0.86 (m, 36H). ^{13}C NMR (100 MHz, $CDCl_3$) δ = 153.6, 143.9, 140.6, 138.9, 138.4, 136.0, 130.8, 129.6, 129.3, 129.0, 126.3, 124.7, 124.0, 123.6, 104.7, 73.7, 69.4, 32.0, 30.5, 20.5, 29.9, 29.8, 29.8, 29.5, 29.5, 26.2, 22.8, 14.2. MS (MALDI-TOF): cald for [M^+]: 3373.30; found: 3373.66. Elemental Analysis cald (%) for $C_{216}H_{330}O_{12}S_8$: C, 76.86; H, 9.85; found: C, 77.22; H, 9.81.

Thermogravimetric analysis

Thermogravimetric analysis was performed with Rigaku Themoplus TC 8120 in air.

Molecular modelling study

Quantum-chemical calculation was performed using Gaussian 2009. Ground-state geometries were optimised at the Becke's three-parameter hybrid functional using the Lee-Yang-Parr correlation functional (B3LYP) level with the 6-31G(d) basis set. For the determination of the molecular length, the molecules were minimised to their ground state with molecular mechanics (MM) under universal force field (UFF).

Characterisation of liquid-crystalline properties

Polarizing optical microscope (POM) Olympus BX51 equipped with a Mettlar FP82HT hot stage was used for visual observations. Differential scanning calorimetry (DSC) measurements were conducted on a NETZSCH DSC204 Phoenix® (Scanning rate: 10 °C min^{-1}). Transition temperatures were taken at the maximum of transition peaks on cooling. X-ray diffraction measurements were carried out on Rigaku RINT 2100 diffractometer Ni-filtered Cu-Kα radiation, which is fitted with a heating stage. For small angle X-ray diffraction, the sample was sandwiched between two polyimide films (Kapton), heated to isotropic state then cooled to the desired temperature for measurement.

Hole mobility measurements

The hole mobilities of LC samples were measured by the time-of-flight (TOF) method. Samples were filled into ITO sandwich cells with a thickness of 9 μm by capillary effects in the isotropic states and were slowly cooled (<1 ˚C min^{-1}) to room temperature to form large planar LC domains. The area of electrodes was measured to be 4 mm × 4 mm. As an excitation light source for excitons generation, a Continuum Electro-Optics MINILITE I (355 nm: the third harmonic generation of Nd:YAG laser) was used. The width of excitation pulses was 5 - 7 ns. The transient photocurrent was observed on a Tektronix TDS 3044B oscilloscope. A DC voltage source, piezo driver (MESS-TEK, M-2647) was used for the generation of an electric field.

UV-vis and fluorescence spectroscopy

UV-vis absorption spectra were recorded on JASCO V-670 fitted with a Mettler FP82HT hot stage**,** fluorescence spectra were recorded on JASCO FP-6500 fitted with a HP-503 hot stage, and integrating sphere fluorescence quantum yield was determined on JASCO FP-8300 with an ILF-835 100 mm diameter integrating sphere attachment. The samples were sandwiched in quartz plates, annealed at 150 ˚C and cooled to room temperature at a rate of 1 ˚C min^{-1} to the desired temperatures. Mechanical shearing was performed with a spatula on the quartz plates.

Preparation of LC gels

Gelators **6** and **7** were first dissolved in chloroform solution. Then each of the solution containing 3 weight% of gelators to **1a** or **1b** was added to LC compounds **1a** and **1b** and the solution was slowly evaporated in air. The resulting mixtures were then annealed at 160 ˚C for 5 minutes before being deposited on glass substrates for optical observations.

Scanning electron microscopy

For scanning electron microscopy (SEM) observations, samples were deposited on glass substrates and the xerogel was prepared by immersing the LC gel mixtures in hexane to extract the LC components and finally dried at room temperature. SEM measurements were performed with a KEYENCE VE-9800 scanning electron microscope.

2. Frontier orbitals study by molecular modelling

The HOMO orbital consists of contributions from the pyrene core itself and the flanking bithiophene groups, whereas the LUMO orbital is contributed by mostly the pyrene core.

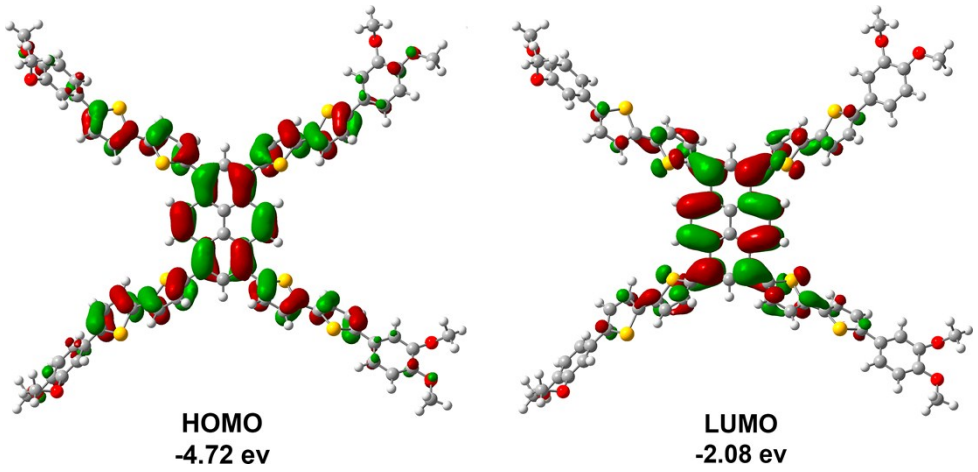

Fig. S1 Computationally calculated frontier orbitals of **1a** by DFT, B3LYP/ 6-31G(d) method.

3. Thermogravimetric analyses

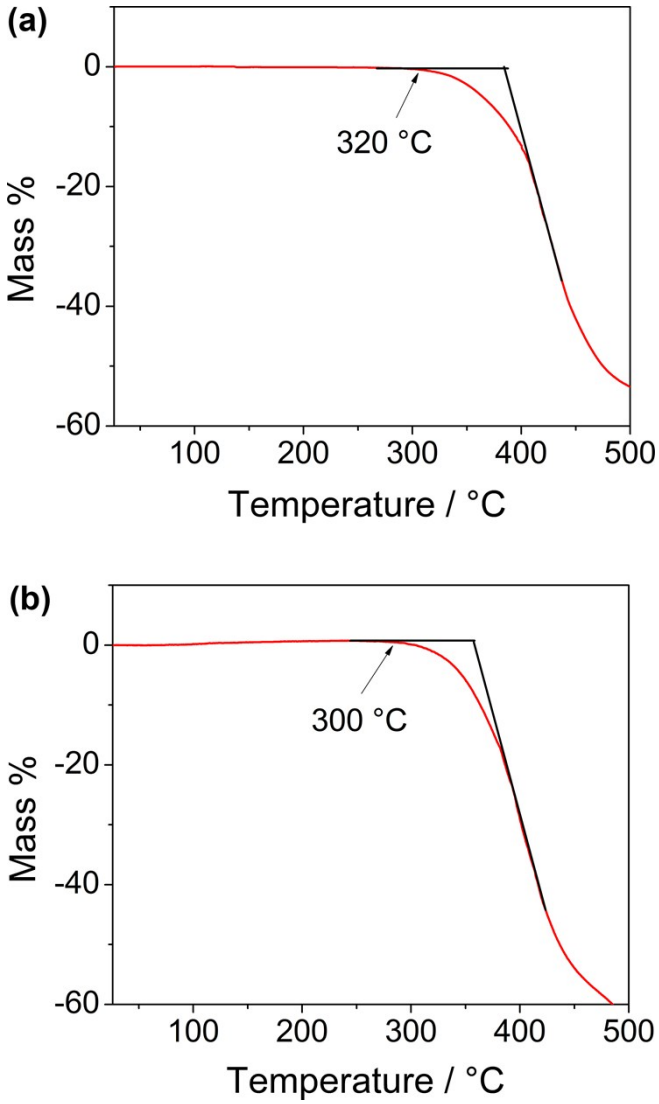

Fig. S2 The thermogravimetric analysis curves for **1a** (a) and **1b** (b).

4. DSC thermograms

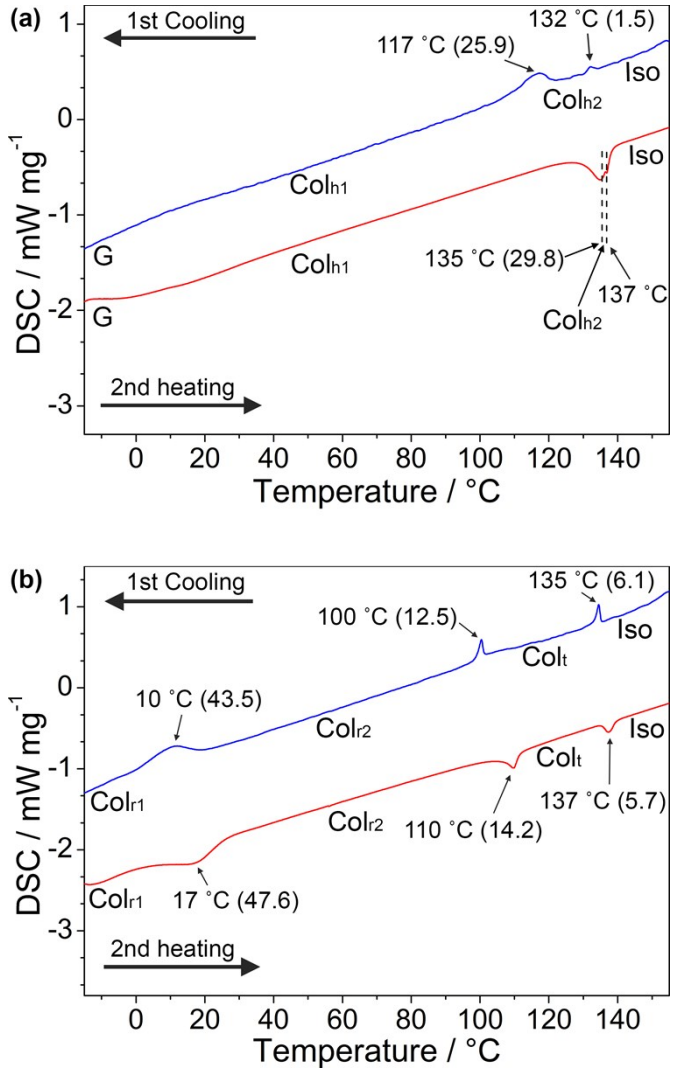

Fig. S3 The DSC traces of compound **1a** (a) and **1b** (b) with a scan rate of 10 K min^{-1}. The transition enthalpy is given in parentheses (kJ mol^{-1}).

5. Additional POM images and X-ray diffraction patterns

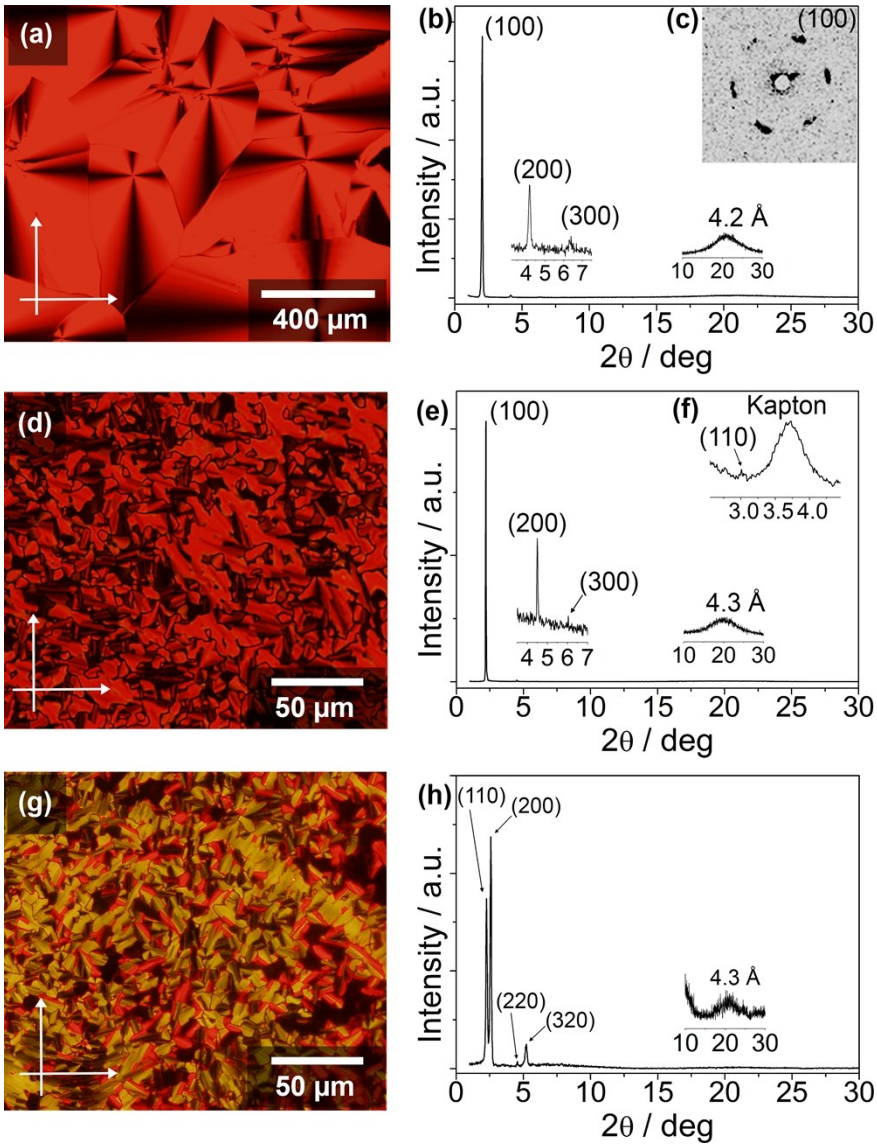

Fig. S4 Polarised optical photomicrographs (left panels) and WAXD patterns (right panels): **1a** in the Col_{h1} phase at 100 ˚C, (a, b) with its two-dimensional SAXD pattern at the same temperature (c). **1b** in the Col_t phase at 125 ˚C (d,e) with its one-dimensional SAXD pattern at the same temperature (f), and **1b** in the Col_{r1} phase at 5 ˚C (g,h).

6. Lattice analyses

Lattice analysis for Col_h and Col_t phases

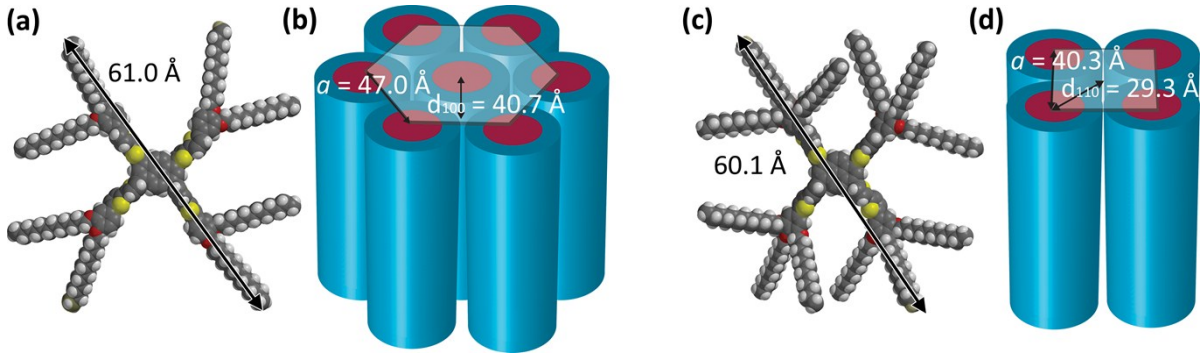

Fig. S5 The edge-to-edge length of a single molecule of **1a** (a), illustration of the Col_h phase of **1a** at 125 ˚C (b), and the edge-to-edge length of a single molecule of **1b** (c), illustration of the Col_t phase of **1b** at 125 ˚C (c).

Lattice analysis for Col_r phase

For an orthorhombic crystal lattice:

$$\frac{1}{d_{hkl}{}^2} = \frac{h^2}{a^2} + \frac{k^2}{b^2} + \frac{l^2}{c^2} \qquad \text{-----} (1)$$

d_{hkl} is the miller indices of a peak assignment, while *a, b* and *c* are the lengths of the lattice on 3 different axes, and they can be represented as d_{100}, d_{010} and d_{001}, respectively. An orthorhombic crystal lattice can be collapsed into a 2D rectangular lattice. Hence:

$$\frac{1}{d_{hk0}{}^2} = \frac{h^2}{a^2} + \frac{k^2}{b^2} \qquad \text{-----} (2)$$

The inter-lattice distance, *d* can be calculated with Bragg's law:

$$n\lambda = 2dsin\theta \quad \text{-----} (3)$$

In this case, λ = wavelength of the incidence X-ray (Cu-Kα, 0.154 nm), θ = incidence angle of the X-ray. Lattice analyses are performed using the Debye Scherer method. The radius of the Debye Scherer ring is obtained by taking the reciprocal of the inter-lattice distance *d*. The radius value is normalized to centimetre scale for simpler analysis.

Assuming a $P2_1/a$ geometry, $d_{200} = a/2$, and d_{110} is essential in determining the value of *b.* Hence d_{110} is substituted into equation (2), and the following equation can be obtained:

$$b = \frac{ad_{110}}{\sqrt{(a^2 - {d_{110}}^2)}} \quad \text{-----} (4)$$

Lattice analysis of 1b at 90 ˚C (Col_{r2})

Table 1 The observed peaks of WAXD of **1b** at 90 ˚C and the corresponding normalised radius of Debye Scherer ring.

Peak No.	2θ	d (Å)	Radius of Debye Scherer Ring (cm)
1	2.059	42.9	2.33
2	2.330	37.9	2.64
3	4.271	20.7	4.84
4	4.812	18.4	5.45

Let d_{110} = 42.9 Å, d_{200} = 37.9 Å, thus a = d_{100} = 75.8 Å. Substituting d = 42.9 Å, a = 75.8 Å into equation (4), b is calculated to be 52.0 Å. Normalised to centimetre scale, 1/a = 1.32 cm, 1/b = 1.92 cm. The Debye Scherer ring can then be plotted (Fig. S6a).

Lattice analysis of 1b at -5 ˚C (Col_{r1})

Table 2 The observed peaks of WAXD of **1b** at 5 ˚C and the corresponding normalised radius of Debye Scherer ring.

Peak No.	2θ	d (Å)	Radius of Debye Scherer Ring (cm)
1	2.245	39.3	2.50
2	2.568	34.4	2.91
3	4.581	19.3	5.19
4	5.222	16.9	5.91

Let d_{110} = 39.3 Å, d_{200} = 34.4 Å. Thus, a = d_{100} = 68.8 Å. Substituting d = 39.3 Å, a = 68.8 Å, b is calculated to be 47.9 Å. Normalised to centimetre scale, 1/a = 1.45 cm, 1/b = 2.09 cm, the Debye Scherer ring is then plotted (Fig. S6b).

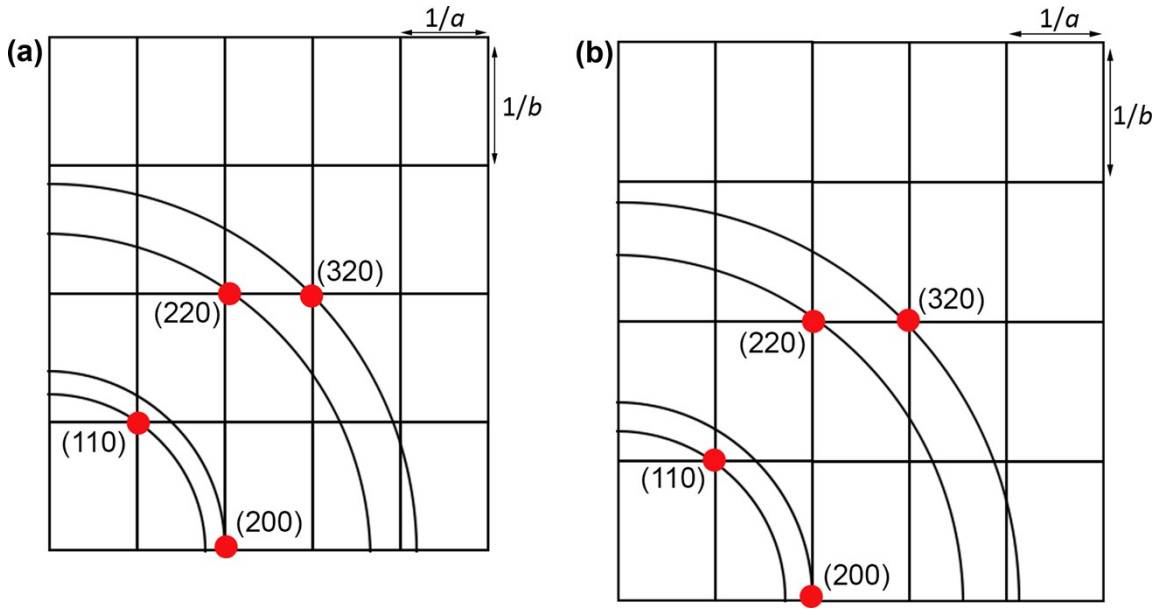

Fig. S6 The Debye Scherer plot of **1b** at 90 ˚C in the Col_{r2} phase (a), and at -5 ˚C in the Col_{r1} phase (b).

Determination of the symmetry of Col_r phase for 1b

The number of molecules in a unit cell (*Z*) can be determined by the following equation:

$$Z = \frac{\rho abc N_A}{M_w} \quad \text{-----} (5)$$

where ρ is the density, *a*, *b*, *c* are the lattice parameters, N_A is the Avogadro's constant, and M_w is the molecular weight.

For Col_{r2} phase of compound **1b** at 90 ˚C, where M_w = 3375.48 g mol^{-1}, *a* = 75.8 Å, *b* = 52.0 Å. Assuming c = 3.0 Å (tilted stacking configuration) and ρ = 1.0 g cm^{-3}, *Z* is calculated to be 2.1.

For Col_{r1} phase of compound **1b** at -5 ˚C, where M_w = 3375.48 g mol^{-1}, *a* = 68.8 Å, *b* = 47.9 Å. Assuming c = 3.0 Å (tilted stacking configuration) and ρ = 1.0 g cm^{-3}, *Z* is calculated to be 1.8.

The presence of the (320) peaks and the value $Z \approx 2$ confirm that Col_{r2} and Col_{r1} phases are of $P2_1/a$ symmetry.

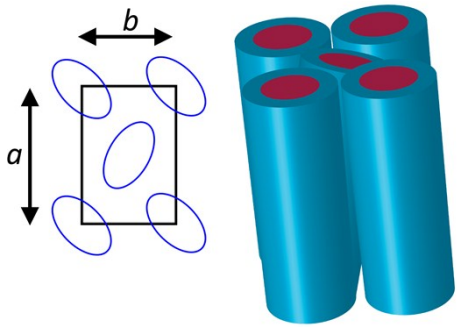

Fig. S7 Illustrations of the $P2_1/a$ symmetry of the Col_{r2} and Col_{r1} phases of compound **1b**.

7. Transient photocurrent curves

The transit time (t_T) of photogenerated holes travelling the LC layer was determined from the inflection point in a double logarithmic plot of transient photocurrent as a function of time. Hole mobility (μ) was calculated from the equation, $\mu = L/(E \bullet t_T)$, where L is the sample thickness and *E* is the electric field strength. This relationship of t_T and *E* is demonstrated in the transient photocurrent curves: As the voltage increases, the transit time decreases accordingly. The hole mobilities of **1a** and **1b** are found to be in the order 10^{-4} and 10^{-5} cm^2 V^{-1} s^{-1}, respectively at room temperature.

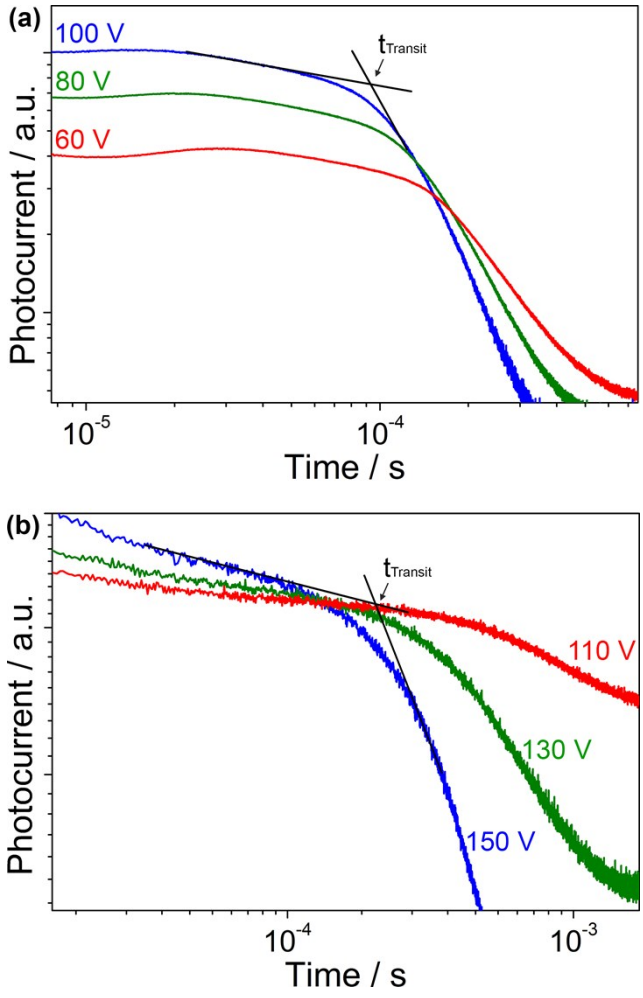

Fig. S8 The double logarithmic plots of the transient photocurrent curves (hole carrier transport) of **1a** (a) and **1b** (b) with respect to applied potential at room temperature.

8. Additional UV-vis and fluorescence spectra

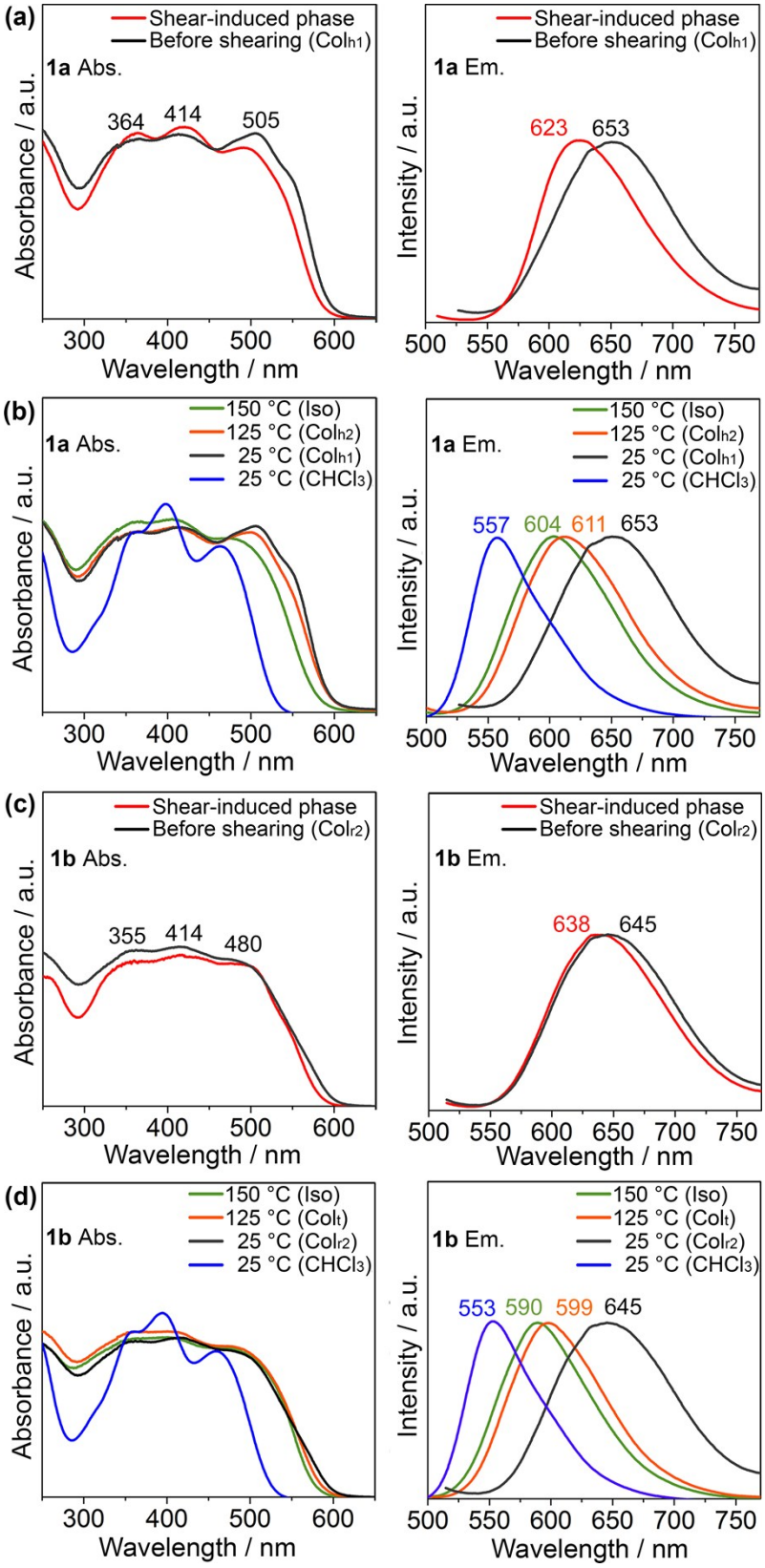

Fig. S9 The normalized UV-Vis absorbance (left panels) and emission (right panels) spectra (excitation wavelength of 420 nm) for **1a** (a, b) and **1b** (c, d). The effect of shearing (a, c), **1a** and **1b** at their various LC and isotropic states, and their solutions in chloroform (2×10^{-5} M) (b, d).

9. Fluorescence quantum yield measurement of 1a

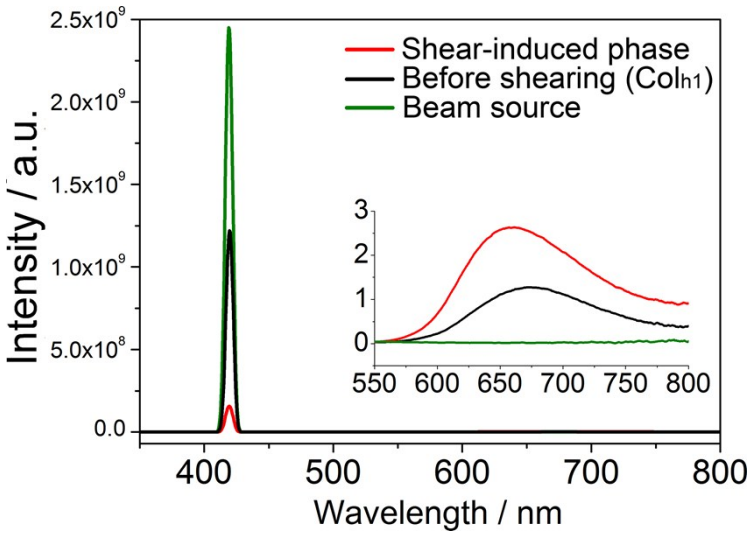

Fig. S10 The integrating sphere fluorescence spectra of **1a** before and after shearing of the sample at room temperature for the determination of absolute quantum yield, with the excitation wavelength of 420 nm.

10. Additional optical microscope and SEM images

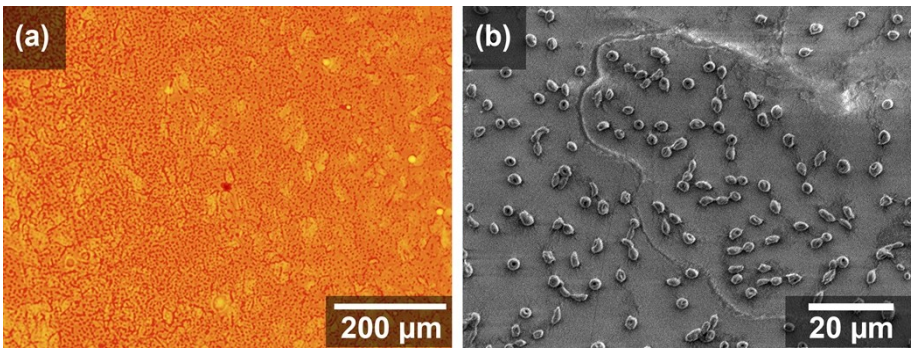

Fig. S11 The images of the mixture of **1a** with gelator **6** under optical microscope at 125 ˚C (a), and under SEM upon removal of **1a** with hexane (b).

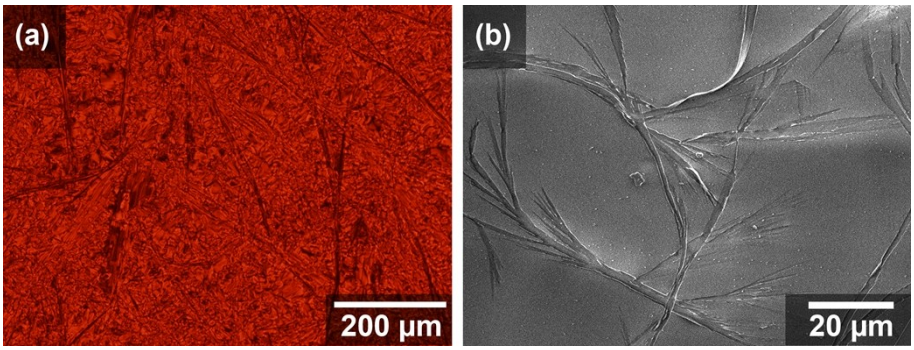

Fig. S12 The images of the LC gel of liquid crystal **1b** and gelator **7** at 125 ˚C under POM (a), and the xerogel under SEM (b).

11. Hole mobilities of LC gels

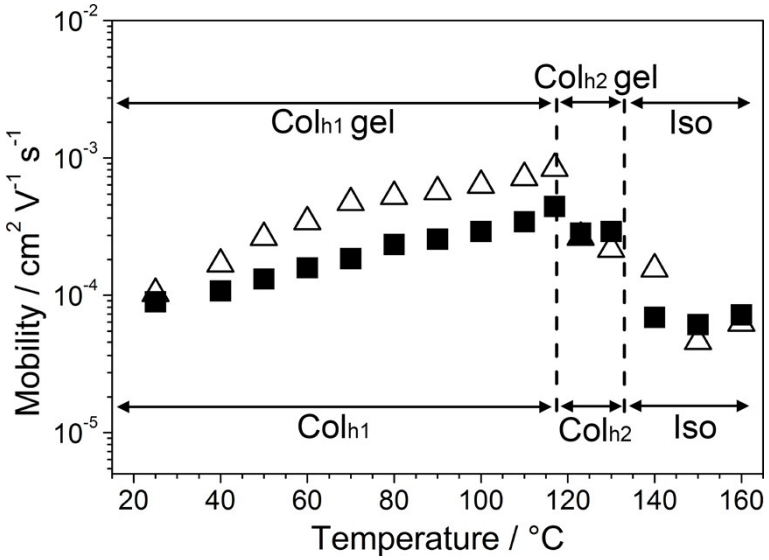

Fig. S13 The logarithmic plot of hole mobilities of **1a** (■) and its LC gel with 3 weight% of gelator **7** (△) as a function of temperature on cooling. Dotted lines denote phase transition temperatures.

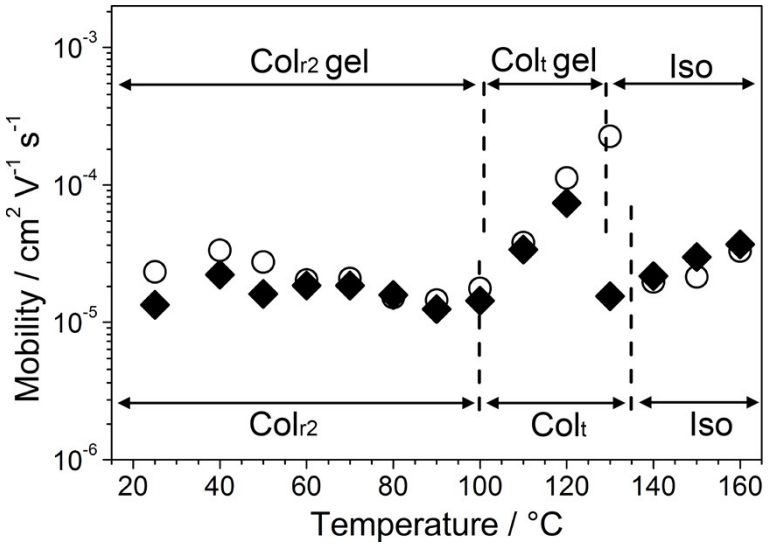

Fig. S14 The logarithmic plot of hole mobilities of **1b** (◯) and its LC gel with 3 weight% of gelator **7** (◆) (b) as a function of temperature on cooling. Dotted lines denote phase transition temperatures.

12. Notes and references

1 B. Zhao, B. Liu, R. Q. Png, K. Zhang, K. A. Lim, J. Luo, J. Shao, P. K. H. Ho, C. Chi and J. Wu, *Chem. Mater.*, 2010, **22**, 435-449.

2 T. Yasuda, T. Shimizu, F. Liu, G. Ungar and T. Kato, *J. Am. Chem. Soc.*, 2011, **133**, 13437-13444.

3 T. Kitamura, S. Nakaso, N. Mizoshita, Y. Tochigi, T. Shimomura, M. Moriyama, K. Ito and T. Kato, *J. Am. Chem. Soc.*, 2005, **127**, 14769-14775.

4 K. Yabuuchi, Y. Tochigi, N. Mizoshita, K. Hanabusa and T. Kato, *Tetrahedron*, 2007, **63**, 7358-7365.

5 K. Tomioka, T. Sumiyoshi, S. Narui, Y. Nagaoka, A. Iida, Y. Miwa, T. Taga, M. Nakano and T. Handa, *J. Am. Chem. Soc.*, 2001, **123**, 11817-11818.